

1 Main Manuscript for

2 Tibetan terrestrial and aquatic ecosystems collapsed with cryosphere loss 3 inferred from sedimentary ancient metagenomics

4
5 Sisi Liu^{a,b*}, Kathleen R. Stoof-Leichsenring^a, Lars Harms^c, Luise Schulte^a, Steffen Mischke^d, Stefan
6 Kruse^a, Chengjun Zhang^e, Ulrike Herzschuh^{a,b,f*}

7 ^aPolar Terrestrial Environmental Systems, Alfred Wegener Institute Helmholtz Centre for Polar and
8 Marine Research, Potsdam 14473, Germany

9 ^bInstitute of Environmental Science and Geography, University of Potsdam, Potsdam 14469, Germany

10 ^cComputing and Data Centre, Alfred Wegener Institute Helmholtz Centre for Polar and Marine Research,
11 Bremerhaven 27570, Germany

12 ^dInstitute of Earth Sciences, University of Iceland, Reykjavík 102, Iceland

13 ^eSchool of Earth Sciences, Lanzhou University, Lanzhou 73000, China

14 ^fInstitute of Biochemistry and Biology, University of Potsdam, Potsdam 14476, Germany

15
16 ***Corresponding author:** Ulrike Herzschuh; Sisi Liu
17 **Email:** Ulrike.Herzschuh@awi.de; Sisi.Liu@awi.de
18
19 **Author Contributions:** U.H. and S.L. conceived this study. S.L. and U.H. led the interpretation and
20 drafted the manuscript. S.L. did the genetic lab work under the guidance of K.R.S. and L.S. S.L. and
21 L.H. performed the bioinformatic analyses with suggestions by K.R.S., L.S. and U.H. S.L. performed
22 the multivariate and network analyses with input by U.H. S.L. and S.K. modeled the paleoclimate
23 change with input by U.H. S.L. simulated the spatio-temporal distribution of permafrost. S.L. performed
24 the data visualization. S.M. and C.Z. performed the fieldwork and provided the samples. All co-authors
25 commented on the manuscript.

26 **Competing Interest Statement:** All authors declare no competing interests.

27 **Classification:** Biological Sciences | Environmental Sciences

28 **Keywords:** ancient metagenomics, lake sediments, ecosystem level, Tibetan Plateau, late
29 Pleistocene/Holocene

30 **This PDF file includes:**

31 Main Text
32 Figures 1 to 3

33 **Abstract**

34 Glacier and permafrost shrinkage and land-use intensification threaten diverse mountain wildlife and
35 affect nature conservation strategy. Our understanding of alpine ecological dynamics is, however,
36 insufficient because time series portraying ecosystem complexity adequately are missing. Here, we
37 present an ancient metagenomic record tracing 317 terrestrial and aquatic taxa, including mammals,
38 fish, plants, and microorganisms retrieved from a lake sediment core from the southeastern Tibetan
39 Plateau covering the last 18,000 years. We infer that steppe-meadow turned into woodland at 14 ka
40 (cal BP) controlled by warming-induced cryosphere loss, further driving a change of herbivore
41 dominance from wild yak to deer. Network analyses reveal that root hemiparasitic and cushion plants
42 are keystone taxa, likely altering the terrestrial ecosystem via facilitation. These findings refute the

43 hypothesis of top-down control by large herbivores in the alpine ecosystem. We also find that glacier
44 mass loss significantly contributes to considerable turnover in the aquatic community at 14 ka,
45 transitioning from glacier-related (blue-green) algae to abundant non-glacier-preferring
46 picocyanobacteria, macrophytes, fish, and fish-eating otters. Human impact contributes little to shaping
47 the alpine ecosystems. By applying network analysis, we provide the first sedaDNA-based assessment
48 of the stress-gradient hypothesis. As cryosphere loss is ongoing due to climate warming, prioritizing the
49 protection of habitats with rich nurse plants that aid neighbors in adapting to stressful conditions is likely
50 to be a more beneficial conservation measure than livestock reduction in the Tibetan Plateau.

51 **Significance statement**

52 Merging ancient metagenomics and network analysis gives new insights into conserving the Tibetan
53 alpine ecosystem under ongoing warming and human perturbations. We investigated the assembly of
54 the Yak steppe-meadow ecosystem and an alpine lake system in response to cryosphere changes over
55 the past ~18,000 years on the Tibetan Plateau. Large herbivores cannot be a cost-effective natural
56 climate solution to stabilize the Tibetan alpine ecosystem because they are not keystone taxa at the
57 ecosystem scale. Furthermore, there is no support that land use considerably shapes the alpine
58 communities and ecosystems. Protection policy should thus prioritize focus on alpine areas with intense
59 land use and rich in root hemiparasitic and cushion plants because these taxa act as facilitators in the
60 ecosystem.

61 **Main Text**

62 **Introduction**

63 High mountain regions harbor a unique biodiversity on which human living and diverse cultures depend
64 (1). To what extent warming, glacier retreat, permafrost thaw, and land use shape the assembly of
65 alpine terrestrial and aquatic communities is heavily debated (2–4). Compared with other mountain
66 areas, upland warming rates are most pronounced on the Tibetan Plateau (5). The glacier and
67 permafrost extent (6), and thereby the world's largest alpine ecosystem, are strongly related to
68 temperature in this region (7, 8). Global warming threatens the unique Tibetan pastoral lifestyles (9)
69 and biodiversity hotspots, such as the Hengduan Mountains on the southeastern Tibetan Plateau (10).
70 Extensive cryosphere loss or even complete disappearance are predicted for the mountains of the
71 eastern Tibetan Plateau by 2100 C.E. (11, 12). Likewise, the Tibetan Plateau lost a substantial part of
72 its cryosphere during the last deglaciation (19–11.7 ka) (13, 14). Hence, discerning the range of
73 ecological responses to past changes of climate, cryosphere, and land use will improve our knowledge
74 and ability to predict future alpine ecosystem changes.

75 Ecological reconstructions, mainly based on pollen data, have documented a shift from alpine steppe
76 to forest-shrub steppe/meadow on the Tibetan Plateau during the late glacial (ca. 14.7–11.7 ka) (15).
77 Hitherto, climate change was assumed to be the main direct driver of this vegetation shift while
78 cryosphere-driven ecological change was not considered. Also, the impact of large wild herbivores as
79 “keystone” species and/or “top-down” engineers, such as ascribed for the Eurasian glacial mammoth
80 steppes (16–18) has not yet been regarded as a major ecological factor for the Tibetan Plateau.
81 Phylogenetic evidence based on modern animals indicates megafaunal migrations and population
82 expansion on the Tibetan Plateau during the late Pleistocene by wild yak (*Bos mutus*), the largest
83 Tibetan herbivore (19). To know whether and to what extent herbivory shaped vegetation in the past is
84 essential for the implementation of “natural climate solutions” to vulnerable ecosystems in the future
85 (20). However, there is no information currently available on megafaunal compositional shifts during the
86 late glacial period on the Tibetan Plateau. It is still unknown whether changes in vegetation respond
87 directly to changes in climate, cryosphere, or megafaunal composition.

88 The earliest human activities at high elevations are dated to 40–30 ka in the Nwya Devu archaeological
89 site (4600 m above sea level/a.s.l.) on the southern Tibetan Plateau (21). Based on archaeological
90 records, year-round habitation at high elevations (> 3500 m a.s.l.) has been widely established since
91 3.6 ka (22). Phylogenetic analyses infer that yak (*Bos grunniens*), the most important herding animal
92 for Tibetans, was domesticated at 7.3 ka and population size increased six-fold between 3.6 and 0 ka
93 (23). Similarly, pollen indicators for livestock grazing such as *Sanguisorba filiformis* and *Rumex*-type
94 are high in records from that time (24, 25). Accordingly, there is an ongoing debate about the extent to

95 which prehistoric land use caused the present Tibetan alpine meadow ecosystem. The mainstream
96 perspective emphasizes that livestock grazing caused the typical Tibetan lawn vegetation (24, 26–28).
97 The alternative viewpoint highlights the importance of abiotic drivers of past and ongoing vegetation
98 change (29, 30). Despite the debate, land management policies aimed at restricting or removing
99 livestock grazing have been strictly implemented at the cost of livelihoods on the Tibetan Plateau over
100 the last twenty years (31). Moreover, since domestic herbivores and their ancestors generally share the
101 same habitats (9), it is hard to distinguish the influence of livestock from that of wildlife grazing on
102 vegetation composition. Accordingly, we still lack basic knowledge on the relative contribution of
103 temperature, the cryosphere, natural herbivory, and land use on vegetation change since the last glacial
104 period. This massively limits our ability to predict ecosystem state shifts and to provide guidance for
105 maintaining and restoring ecological functions.

106 Likewise, little is known about the long-term changes of Tibetan Plateau lake communities, including
107 macrophytes (32, 33), microbes, fish, and mammals, although the Tibetan Plateau is rich in lakes which
108 represent unique biodiversity hotspots (34). Most studies suppose a direct response of aquatic
109 organisms to lake-water levels (attributed to climate changes) during the late glacial period (32, 35, 36).
110 Recently, some studies argue that glaciers, via runoff, directly contribute to a lake's microbial
111 composition as revealed by aquatic biomarker (n-alkanes) concentrations from Lake Hala Hu
112 (northeastern Tibetan Plateau) (37) and microbial sedimentary DNA from Lake Yamzhog Yumco
113 (southern Tibetan Plateau) (38). However, there is little knowledge of shifts in aquatic communities,
114 particularly how those taxa poorly represented in the (micro-)fossil records responded to climate
115 changes and related glacier retreats. Furthermore, during the late Holocene, human impacts on lake
116 ecosystems are frequently inferred from a few taxa in individual assemblages such as zooplankton,
117 algae, and submerged macrophytes. There is thus a knowledge deficit on the extent to which glacier
118 dynamics and human-relevant activities contribute to ecosystem-level turnover in high-alpine
119 environments.

120 Temporal species co-occurrence (co-existence) information is required to understand species assembly
121 processes, including environmental filtering and biotic interactions (39, 40). According to the stress-
122 gradient hypothesis – a major concept in ecology – positive interactions between species will become
123 more common as environmental stress increases (41). For instance, facilitation is repeatedly reported
124 to support the persistence of terrestrial alpine plants via microclimatic modifications from cushion plants
125 (42, 43), a conclusion with high relevance when climate is warming (44). Those cushion plants such as
126 *Saussurea* and *Saxifraga* are characterized by a ground-hugging mat or dense stem structure, enabling
127 them to trap heat and soil while also providing habitable conditions for other species within their crown
128 area. However, aside from vegetation, the stress-gradient hypothesis has been little investigated at the
129 ecosystem level. Even more, studies supporting this hypothesis almost exclusively originate from
130 space-for-time assessments despite species assembly being a dynamically complex process. Further,
131 other studies from the Tibetan Plateau have shown that major ecosystem attributes such as plant
132 richness are not analogous in space and time (45).

133 Lake sediments are the most suitable archives for tracking temporal species-environment relationships
134 (46). Compared to the traditional proxies (e.g., pollen and diatoms), sedimentary ancient DNA (sedaDNA)
135 extracted from lake sediments has become a powerful tool for retrieving more detailed assemblage of
136 past plants, animals, and microbes within lakes and their catchments (47). SedaDNA metagenomics
137 (shotgun sequencing) has been increasingly used for ecosystem-level investigations and shows reliable
138 taxonomic classification down to the genus level due to advancements in bioinformatic analysis and
139 reference databases (48, 49). To date, times-series studies of lake sedaDNA studies investigating taxa
140 composition and co-occurrence at the ecosystem level are not available for the Tibetan Plateau.

141 We reconstruct terrestrial and aquatic communities by shotgun sequencing on 40 sedaDNA samples
142 covering 17.7–0 ka extracted from Lake Naleng, located in the Hengduan Mountains, southeastern
143 Tibetan Plateau (Fig. 1A). Its surrounding landscape has been influenced by Quaternary glaciation
144 and/or permafrost (Fig. 1A, B, and *SI Appendix*, Fig. S1). The sedaDNA results reveal diverse mammals
145 with a dominance of bovid species (e.g., wild yak) in the pre-14 ka period when steppe-meadow was
146 well established. The Yak steppe-meadow ecosystem collapsed at 14 ka and shifted to woodlands
147 supporting cervid species (e.g., red deer). No evidence supports large wild herbivores' "top-down"
148 control of vegetation shifts. Rather, warming-induced cryosphere loss directly triggered the vegetation
149 changes that further forced the mammalian composition turnover. Likewise, we find that glacier mass
150 loss at 14 ka strongly shaped the aquatic ecosystem from glacial microbes to a variety of interglacial

151 organisms such as picocyanobacteria, submerged plants, fish, and otters. Overall, we infer only a
152 limited impact of land use. After 3.6 ka, land use may have reduced mammals' occurrences and
153 contributed to the establishment of a picocyanobacterial turbid lake system. Through network analysis,
154 partial correlations, controlling the influence of cryosphere changes, land use, and mediator taxa, act
155 as surrogate representations of the direct associations among taxa. We find a high number of positive
156 links during the glacial period (pre-14 ka, a high-stress phase) in both ecosystems, directly supporting
157 the stress gradient hypothesis over a long time span.

158 **Results and Discussion**

159 **Ecosystem-level sedaDNA record of the past terrestrial and aquatic biosphere**

160 Sequencing yielded 2,512,713,391 reads for bioinformatic analyses, of which 123,786,174 reads came
161 from 40 samples and 12 controls which underwent taxonomic data cleaning and filtering (Materials and
162 Methods, *SI Appendix, Supplementary Text*). Consequently, 1,067,557 reads of 317 terrestrial and
163 aquatic taxa, comprised of seed-bearing plants, mammals, macrophytes, fish, algae, and
164 Cyanobacteria (also called blue-green algae), with best identity $\geq 95\%$ against the NCBI Reference
165 Sequence Database were used for ecosystem reconstruction. The ancient origin of the reads was
166 confirmed by read length distribution (*SI Appendix, Fig. S2*) and characteristic C-to-T substitution at the
167 5' and 3' end with sufficient reads (Materials and Methods, *SI Appendix, Fig. S3 and Fig. S4*)

168 The shotgun sequencing approach recovered 167 genera from 81 families of seed-bearing plants (*SI*
169 *Appendix, Datasets 1*). Among these, the dominant ones are species-rich on the Tibetan Plateau and
170 are also abundant and detected by metabarcoding and pollen analyses (25, 45, 50) from the same
171 sedimentary core (*SI Appendix, Table S1*). The mammals, which have less biomass than plants, were
172 traced by the shotgun sequencing approach in all samples (*SI Appendix, Datasets 1*). Most mammalian
173 reads were identified to even-toed ungulate mammals such as Bovidae and *Cervus*, followed by
174 *Ochotona*, a rodent-like mammal dwelling on mountains. For aquatic communities (*SI Appendix,*
175 *Datasets 2*), the reads assigned to genera of aquatic macrophytes are abundant in *Potamogeton*
176 (*Potamogetonaceae*) and *Myriophyllum* (*Haloragaceae*). *Salmonidae* and *Cyprinidae* dominated the
177 fish assemblage, with *Cyprinidae* being more abundant in the high-elevation regions of the current
178 Tibetan Plateau (51). Few reads were classified to *Lutra*, which is currently one of the endangered top
179 predators in aquatic ecosystems (52). Most algal reads were assigned to *Monodopsidaceae*,
180 specifically its genera *Nannochloropsis*, which contains species that can adapt to harsh environments
181 such as the Last Glacial Maximum (53). As cyanobacterial blooms relate to lake ecosystem health (54),
182 we focus on bacterial reads assigned to genera and families of Cyanobacteriota, among which
183 *Leptolyngbya*, *Pseudanabaena*, and *Synechococcus* are the dominant genera.

184 Our results indicate, for the first time, that a single shotgun dataset can depict the biotic community at
185 an ecosystem level. Our results further indicate that terrestrial and aquatic changes can concurrently
186 be traced using the same approach. Even more, our time-series data suggest that a more continuous
187 proxy signal can be retrieved from lake sediments compared with, for example, permafrost sediments
188 (55). This is despite the fact that the majority of cellular organisms' reads (98.6%) did not match any
189 Eukaryota, which is consistent with previous environmental shotgun studies (56–58): even a small
190 proportion of the reads (1.4%) can provide a significant amount of taxonomic information. The value of
191 our dataset may increase in the future when more comprehensive databases are used for taxonomic
192 assignment.

193 **Terrestrial ecosystem shifts from late glacial Tibetan Yak steppe-meadow to Holocene deer 194 woodland**

195 Overall, our results indicate an abrupt collapse of alpine steppe-meadow at 14 ka, followed by advance
196 of subalpine shrubland during 14–3.6 ka and alpine steppe-meadow re-expansion since 3.6 ka (Fig. 2A
197 and B).

198 The pre-14 ka vegetation is characterized by alpine forbs and graminoids including taxa dominant today
199 in cold-dry places (e.g., *Saxifraga*, *Asteraceae*, and *Poaceae*), on moist stream banks and in meadows
200 (e.g., *Carex*, *Pedicularis*, and *Ranunculaceae*) of the Tibetan highlands. During 14–3.6 ka, the
201 abundance of woody taxa increased, with the main components being the *Salicaceae* taxa (e.g., *Salix*)
202 and *Rhododendron*, as well as a portion of *Picea* during 10–3.6 ka (Fig. 2B). Although *Salix* is usually

203 over-represented in sed(a)DNA spectra, its high values together with *Rhododendron* well reflect the
204 subalpine shrub communities of the eastern Tibetan Plateau (59). Since 3.6 ka, the abundance of some
205 forbs and graminoids (e.g., Asteraceae, Polygonaceae, and Poaceae) increased (Fig. 2A) even though
206 woody taxa (e.g., Salicaceae and *Rhododendron*) were still abundant. Accordingly, the lake catchment
207 experienced a cold-dry climate during the glacial period, followed by a moderate-to-warm and moist
208 climate between 14 and 3.6 ka, and then returned to cold conditions afterward. The main vegetation
209 characteristics and climate conditions agree with studies of metabarcoding and pollen analyses from
210 the same sedimentary core (SI Appendix, Fig. S5A) as well as regional pollen records (SI Appendix,
211 Fig. S5B).

212 Our shotgun data indicate that the main terrestrial mammals are medium- to large-sized ungulate
213 herbivores (> 45 kg, Fig. 2C and D). In general, mammalian composition shifted from the steppe-
214 meadow-adapted bovid community in the pre-14 ka period (Fig. 2A and C) to a mesic-adapted
215 woodland cervid community post-14 ka (Fig. 2B and D). However, a compositional shift back did not
216 co-occur with steppe-meadow re-establishment during the late Holocene (Fig. 2A and C). In the pre-14
217 ka period, herbivores (*Bos* and other bovids) that currently inhabit alpine ecosystems in the northern
218 and western plateau were abundant. *Ochotona* (pika), which shares similar habitats, occurred as well
219 (Fig. 2C). In the post-14 ka period, *Cervus* occurred (Fig. 2D); while all Bovidae species had very low
220 proportions except for evidently increased numbers at 3.5 ka only (Fig. 2C). Meanwhile, our data also
221 record a higher amount of Cricetidae sedaDNA after 14 ka (Fig. 2E) – which frequently occurs in the
222 present-day moist meadows on the Tibetan Plateau. To our knowledge, this is the first sedaDNA record
223 of the mammalian community on the Tibetan Plateau.

224 We investigated the key drivers of compositional changes for plants and mammals at the terrestrial
225 community level using constrained ordination analyses (Materials and Methods). Assessed drivers
226 include cryosphere (Fig. 2F and G, permafrost and glacier distribution simulated using temperature
227 change and validated by sedaDNA-based permafrost and glacier microbiota changes, see Materials
228 and Methods), herbivory (Fig. 2H, *Bos*%, excluded for mammalian constrained ordination), land use
229 (Fig. 2I, *Rumex* and *Sanguisorba*%, ref. (24, 25)), and vegetation (Fig. 2J, PC1 of PCA site score,
230 excluded for vegetation constrained ordination). All variables together explain a high amount of variation
231 in the vegetation composition (Fig. 2K, 73%, $P = 0.001$). Variation partitioning (Fig. 2K) indicated that
232 the cryosphere alone explains most of the vegetation variation (34.4%, $P = 0.001$) compared with the
233 variance exclusively explained by herbivory (0.1%, $P = 0.246$) and land use (1.2%, $P = 0.011$). Such
234 results give no support for the hypothesis of a “top-down” regulated plant community by large herbivores
235 (16, 17). Furthermore, we find that the compositional change of mammals is strongly explained by
236 vegetation changes (64.2%, $P = 0.001$) and cryosphere (unique 61.1%, $P = 0.001$) but poorly by land
237 use (unique 1.8%, $P = 0.051$, Fig. 2K). Accordingly, the millennial-scale findings undermine the long-
238 term argument of a human-driven ecosystem change on the Tibetan Plateau at a millennial time scale
239 (28, 60).

240 An increasing number of studies have reported that co-occurrence networks can offer more information
241 than composition on community organization, and a few studies have focused on the ecosystem level
242 (61). We investigated species' co-occurrence patterns at the ecosystem level (Methods and Materials)
243 to understand direct interactions (e.g., facilitation and competition) among coexisting taxa in two
244 different regimes, pre-14 ka (high stress) and post-14 ka (low stress). We specifically focus on positive
245 partial correlation as an indicator of facilitation among taxa. Our aim is to assess the applicability of the
246 stress gradient hypothesis on a millennial scale. This assessment serves as an analogy for
247 understanding shifts in facilitation within the context of ongoing cryosphere loss and land-use changes
248 in mountain regions.

249 The whole terrestrial community is clustered into two modules (Fig. 2L) by taking cryosphere changes
250 and land use as predictors (SI Appendix, Fig. S6A), separating common taxa of the pre-14 ka
251 community (e.g., Asteraceae, Bovidae, and *Ochotona*) from those dominating the post-14 ka
252 community (e.g., *Salix*, *Cervus*, and Cricetidae). The percentage of positive links within the terrestrial
253 community is higher in the pre-14 ka period compared with the post-14 ka interval (76% and 61%,
254 respectively, Fig. 2L). This strongly supports the stress-gradient hypothesis (61) which proposes that
255 positive interactions are promoted under stressful conditions such as the cold glacial period in our study.
256 Furthermore, we used Kleinberg's hub centrality score, which ranges from 0 to 1, to identify the keystone
257 taxa, as it measures the extent of a taxon's connections to other important taxa in the overall network
258 (62). A taxon with a high hub centrality score is more likely to be a keystone taxon that is particularly

259 important to the functioning of ecosystems (63, 64). We find that Bovidae and *Bos* (wild yak) show lower
260 Kleinberg's hub centrality scores (0.76 and 0.623) than their main food resources in their respective
261 modules (Asteraceae: 1; Poaceae: 0.9, *SI Appendix*, Table S2), thus refuting the hypothesis of large
262 herbivores as keystone taxa in the Tibetan terrestrial ecosystem.

263 A major finding is that the cryosphere governed the terrestrial Tibetan ecosystem characteristics until
264 14 ka by promoting a forb-dominated steppe-meadow (Fig. 2K) that spread in the glacier-free catchment
265 areas on permafrost soils (Fig. 1B and *SI Appendix*, Fig. S1). Our results furthermore suggest that such
266 steppe-meadow composition was “bottom-up” controlled, with plants such as *Pedicularis*, *Saxifraga* and
267 Asteraceae species as keystone taxa, as indicated by their high Kleinberg's hub centrality scores (Fig.
268 2L and *SI Appendix*, Table S2). *Pedicularis*, a root-hemiparasitic genus, can enhance grassland
269 diversity by reducing the competitive advantage of grasses and legumes (which are preferred hosts)
270 compared to forbs and sedges on the Tibetan Plateau (65). Asteraceae contain a variety of genera that
271 form cushions (e.g., *Saussurea* and *Senecio*), which can protect diverse terrestrial alpine plants against
272 the harsh environment on an ecosystem level by creating a favorable microclimate through their dense,
273 low-lying cushion structure, as well as stabilizing soil, retaining water, and contributing to nutrient cycling
274 (43, 66). Similar to *Saxifraga*, the cushion life form contributes to the diversification of other species-
275 rich alpine genera in the Tibetan Plateau (67). These findings indicate that facilitation rather than
276 competition shaped the glacial terrestrial Tibetan ecosystem. It represents a first assessment of the
277 stress-gradient hypothesis over millennial time scales.

278 A further key finding suggested by our shotgun data is that abundant large herbivores such as wild yaks
279 co-occurred with grass- and forb-dominated steppe-meadow (Fig. 2A, and C) extending across
280 permafrost soils (Fig. 2F). This suggests that they frequently consumed protein-rich forbs rather than
281 exclusively or heavily depending on grasses (68). The Lake Naleng's non-pollen palynomorphs (NPP)
282 record supports this inference, indicating high percentages of *Glomus* before 14.5 ka (69). Given their
283 association with erosion events and the fact that their hosts, such as Asteraceae are frequently
284 consumed by yaks in winter, an increased input of *Glomus* spores might originate from the dung of
285 bovids after foraging on these plants (70, 71). Such consumers' preferences are similar to the Eurasian
286 “mammoth steppe” supporting a variety of mammals during the late Pleistocene in high latitudes (58,
287 72). Furthermore, vegetation shifts drive changes in mammalian communities in our study area
288 (explained 64.2%, Fig. 2K), which may emphasize that resource stress (e.g., less available foraging
289 habitats) could also pressure herbivores to facilitation rather than competition (positive partial
290 correlations among mammals in the post-14 ka, Fig. 2L) which is typically less considered (73).

291 Overall, we suggest that temperature-driven cryosphere changes (Fig. 2F and G) controlled vegetation
292 turnover on the Tibetan Plateau at 14 ka, which in turn promoted a decline of large herbivory. This
293 contrasts with the proposition of megafauna as keystone engineers of the “Mammoth steppe”
294 ecosystem of Glacial Siberia (74). Our permafrost simulation using a generalized linear model (Methods
295 and Materials) shows that permafrost thawed at 14 ka in the U-shaped valley around Lake Naleng and
296 along streams in response to the warming climate (Fig. 1B and *SI Appendix*, Fig. S1) and this is
297 confirmed by time-series data for permafrost bacteria (*SI Appendix*, Fig. S7A-C). This likely promoted
298 the development of alluvial soils, thereby facilitating riparian woody vegetation (*Salix* sp.) (75) as
299 indicated in our sedaDNA record. This vegetation change may have limited the protein intake of large
300 herbivores (e.g., yaks) (76), presumably forcing them to migrate to the restricted permafrost upslope or
301 farther away to the northeastern Tibetan Plateau, where forbs still dominate today (15). Similarly, a
302 decline of megafaunal grazers is reported to be coeval with dwarf willow expanding northward into the
303 “Mammoth steppe” of northeast Siberia and North Alaska around 14.5–13.5 ka (77).

304 Another major result of our study suggests that cryosphere changes and not human impact (Fig. 2K)
305 were the main driver of terrestrial ecosystem change on the Tibetan Plateau at a millennial time scale.
306 Even the partial re-establishment of steppe-meadow during the late Holocene (Fig. 2A), which has often
307 been related to human impact (e.g., livestock grazing, ref. (28)) could be best explained by cooling-
308 related permafrost re-establishment in the upper Lake Naleng catchment area. Unexpectedly, a steady
309 re-occupation by Bovidae species such as wild yak did not co-occur with the re-establishment of steppe-
310 meadow habitats (Fig. 2A and C), nor did our record indicate any substantial herding activity post-3.6
311 ka. This contrasts with the co-abundance of bovid taxa and grassy alpine taxa pre-14 ka. Although crop
312 agriculture was introduced into the southeastern Tibetan Plateau and spread up to 3600 m a.s.l. from
313 3.6 ka (22), cold and dry weather in this area probably forced the farmers to supplement their diets by

314 hunting wild animals (78) and this may have contributed to a herbivore decline in contrast to the inferred
315 high population levels associated with the pre-14 ka analog vegetation composition.

316 **Aquatic ecosystem shifts from a glacially impacted microbial system to a warm macrophyte**
317 **fish-otter system**

318 The aquatic ecosystem is characterized by a microbial community dominated by green algae and
319 cyanobacteria during the cold, glaciated period before 14 ka (Fig. 3A), by the co-occurrences of
320 picocyanobacteria and submerged macrophytes, fish, and otters during the warm and glacier-free early
321 and mid-Holocene (Fig. 3B, C, and D), and by the dominance of non-glacially adapted
322 picocyanobacteria after 3.6 ka (Fig. 3B). Evaluated drivers include glacier mass (Fig. 3E) and land use
323 (Fig. 3F, *Rumex* and *Sanguisorba*%, ref. (24, 25)), which explain 61% ($P = 0.001$) of the variation of the
324 aquatic communities at the ecosystem level. Variation partitioning indicates that compositional turnover
325 is strongly related to glacier mass changes (47.5%, $P = 0.001$, Fig. 3E), followed by land use (6.6%, P
326 = 0.001, Fig. 3F). These findings suggest that glacier dynamics may be the main driver of the lake's
327 community composition change on the Tibetan Plateau (37, 38).

328 Network analyzes taking glacier mass changes and land-use as predictors group aquatic taxa into two
329 modules (Fig. 3G), typified by a unique community in the pre-14 ka period (e.g., *Nannochloropsis*,
330 *Pseudanabaena*, and *Anabaena*) and post-14 ka (e.g., *Myriophyllum*, *Triphlophysa*, *Salmonidae*,
331 *Poeciliidae*, *Percidae*, and *Planktothrix*). The aquatic ecosystem exhibited a higher relative number of
332 positive links in the pre-14 ka period (Fig. 3G), supporting the stress gradient hypothesis. Apart from
333 glacier loss, land use drives partial correlations among taxa (SI Appendix, Fig. S6B), suggesting that
334 Lake Naleng's productivity and nutrient status play a role in co-occurrence pattern of the whole lake
335 ecosystem.

336 Lake community inferred from shotgun data was dominated by microbial taxa, including
337 *Nannochloropsis* (green algae), *Leptolyngbya*, and *Pseudanabaena* until 14 ka (Fig. 3A), when the lake
338 catchment became glacier-free (Fig. 3E). These taxa or their congeners are known from cryoconite
339 holes on a glacier's surface in the Arctic and Asian mountains (79) and have been retrieved from Arctic
340 lake sediments from the glacial period (53). Our results confirm that a glacier's microbial communities
341 are able to colonize downstream, and that glacier ecosystem changes can be traced by lake sediments
342 (80–82). Further, the high relative abundance of *Oscillatoria*, the genera hosting rich toxin-producing
343 strains (54, 83), in the pre-14 ka period (Fig. 3A) possibly forced microbes into engaging in positive
344 associations (84, 85). Yet, whether such biotic-relevant stressors can trigger lake communities to
345 interact positively and override the effects of abiotic stress (e.g., glacier) on millennial scales will require
346 further evaluation.

347 Obviously, glacier disappearance (Fig. 3E) induced a transition from glacier-preferring (blue-green)
348 algae in the pre-14 ka period to picocyanobacteria communities during post-14 ka, including the
349 *Synechococcus* and *Cyanobium* taxa (Fig. 3B). Their relative abundance declined when other
350 submerged plants such as *Potamogeton*, *Stuckenia*, and *Myriophyllum* (Fig. 3C) notably increased in
351 response to warmer water conditions (86), which, in turn, favored the invasion from lower elevations
352 and successful reproduction of fish (87, 88) including *Salmonidae* and *Cyprinidae* (Fig. 3D). These fish
353 promoted the establishment of piscivores including otters (89). In addition, the submerged macrophytes
354 can efficiently maintain water quality by releasing anti-cyanobacterial fatty acids (90). The key roles of
355 submerged plants and fish are further inferred from co-occurrence patterns (SI Appendix, Table S3).

356 Two lake states likely coexist in one aquatic ecosystem post-14 ka, either spatially (SI Appendix,
357 *Supplementary Text*) or temporally separated, i.e., a macrophyte-dominated clear-water lake system at
358 the lake shore and a blue-green algae-dominated turbid lake system. Hence a complex subalpine lake
359 ecosystem was established during the warm phase (post-14 ka) characterized by a low degree of
360 centralization (Fig. 3G). Probably initiated by a decline in temperature-lowering submerged
361 macrophytes, the lake ecosystem completely collapsed, leaving picocyanobacteria (*Synechococcus*
362 and *Cyanobium* taxa, Fig. 2B) as the main component, which, in turn, posed a further threat to
363 submerged plants by reducing light and oxygen (91). To what extent this change was enhanced by
364 human impact is uncertain but it is rather unlikely as we find no clear traces of herding (e.g., livestock
365 DNA) in the mammalian community (Fig. 2C and D). This finding highlights the importance of taking a
366 long-term perspective when assessing the effects of natural and human-induced factors on lake state

367 transitions, particularly before predicting the presence of critical transitions (92) and implementing
368 sufficient lake restoration strategies to mitigate cyanobacteria blooms (54).

369 **Conclusions and lessons learned for risks in a warmer future and restoration if temperatures
370 cool again**

371 We find that climate and cryosphere-induced vegetation changes impact mammal abundance and
372 composition, not vice versa; hence, there is no support for herbivory as a major ecosystem driver.
373 Accordingly, managing large herbivores may not represent a conservation option; instead, only lowering
374 the temperature by reducing global carbon emissions and preserving the cryosphere will help the
375 conservation or restoration of the Tibetan alpine ecosystem.

376 We infer that *Pedicularis* and cushion plants (Asteraceae and *Saxifraga*), in particular, are keystone
377 taxa for the Yak steppe-meadow ecosystem and should accordingly be the focus of protection
378 measures, as they support high biodiversity at the ecosystem level by common facilitations. The way
379 to protect them is to conserve their habitats, with priority given to areas not invaded by shrubs.

380 We deduce that greater grazing during the late glacial compared with the late Holocene did not
381 destabilize the terrestrial ecosystem. By analogy, relaxed pasture management (e.g., moderate
382 livestock reduction policy) does not represent a risk to the present Tibetan Plateau ecosystem but can
383 be recommended to sustain contemporary livelihoods in the highlands of the Tibetan Plateau (93).

384 Pronounced shifts in the dominance of aquatic taxa, particularly microbial communities, occurred
385 synchronously with the substantial decay of glaciers at 14 ka, whilst the glacial lake ecosystem was not
386 restored in the cold late Holocene (3.6–0 ka) presumably because glaciers did not re-establish. Our
387 findings call for more effort to inspect the glacier-lake connectivities of microbial communities as a base
388 for developing and implementing appropriate conservation strategies. However, it is important to note
389 that the specific aspects of glacial microbes that should be protected may vary depending on the
390 ecosystem and the goals of conservation efforts. As our study does not investigate this aspect, we
391 cannot offer specific recommendations for conservation actions related to glacial microbes in Tibetan
392 glacial lakes.

393 Warmth-related aquatic ecosystems composed of submerged macrophytes and blue-green algae
394 support fish and otters (main predators of fish). Warmth increased the complexity of the lake ecosystem
395 with the coexistence of two states and less common positive associations. The lake ecosystem shifted
396 to a turbid water state with few eukaryotes primarily due to cold-related macrophyte loss. It is unlikely
397 that the external loading of nutrients (e.g., from husbandry) caused such a state shift as no similar signal
398 has been observed from the terrestrial mammalian community.

399 We find that terrestrial and aquatic species co-occurrence patterns respond to the loss of the Tibetan
400 cryosphere. A structure with fewer facilitative interactions suggested by positive partial correlations was
401 detected for a permafrost-free terrestrial ecosystem and a glacier-free aquatic ecosystem. Our findings
402 have broader implications beyond our study site, as we investigated a typical alpine lake with a
403 catchment that includes elevational ranges typical of the southeastern Tibetan alpine ecosystem.

404 **Materials and Methods**

405 **Modern site setting**

406 Lake Naleng (31.10° N, 99.75° E; 4200 m a.s.l.) is situated in a glacier-formed basin on the southeast
407 Tibetan Plateau, which is a biodiversity hotspot (also referred to as the Hengduan Mountains). This lake
408 is classified as a mesotrophic lake based on its pH-value (8.11), Secchi depth (2.9 m), and dissolved
409 oxygen content (6.86 mg/l) (measured at noon in 09.2009, ref. (69)). The catchment area is about 120
410 km² and characterized by steep slopes and a narrow floor (U-shaped glacial trough) with Miocene
411 granite and granodiorite rocks (94). The study area is mainly influenced by the South Asian summer
412 monsoon and the East Asian winter monsoon. Warm and humid air masses occur in summer whilst
413 cold and dry air masses dominate in winter. The modern catchment vegetation is alpine shrubland and
414 meadow with two patches of forests on mountain slopes (SI Appendix, Supplementary Text). Human
415 influence is livestock grazing (yaks and Tibetan sheep) in alpine meadows during the summer in the
416 lake catchment (25).

417 **Late Pleistocene/Holocene site setting**

418 The regional and local climate was generally cold and dry during the late glacial period (15), with
419 moraines in the lake's outlet dating to 21.5–17.5 ka (95), suggesting glaciers shaped the lake basin
420 during and even earlier than this period. During the Holocene, a warm and humid climate has been
421 widely recorded for the southeastern Tibetan Plateau (96) as well as our lake catchment (25, 94). These
422 environmental settings are well captured by our cryospheric simulation (*SI Appendix, Supplementary*
423 *Text*) and sedaDNA metagenomics (*SI Appendix*, Fig. S7A and B). Human impacts are assumed to
424 have intensified at high elevation when the agropastoral economy expanded up to 3500 m a.s.l. around
425 3.6 ka (22). Based on the C/N ratios (varying between 2 and 16) and $\delta^{13}\text{C}_{\text{org}}$ values (varying between -
426 31% and -25%) of the Naleng core (94), it is suggested that the lake sediments primarily contain the
427 remains of aquatic organisms, and have received very little input of terrestrial plant materials through
428 time (97).

429 **Core, chronology, and sedimentary ancient DNA material**

430 The core collection, dating, and age-depth model are described in a previous study (69, 94). Due to a
431 lack of macrofossils, sixteen samples of bulk organic carbon were dated by accelerator mass
432 spectrometer (AMS) ^{14}C at the Leibniz Institute Kiel.

433 The 1 cm thick sediment samples were stored at 4°C until subsampling for sedaDNA isolation that was
434 performed using a PowerMax® Soil DNA Isolation kit (Mo Bio Laboratories, Inc. USA) with a modified
435 protocol. A full description of the procedures is provided in Liu et al. (45).

436 **Library preparation and shotgun sequencing**

437 A total of 40 sedimentary ancient DNA samples spanning 17.7–0 ka was used for library preparation.
438 Each library batch contains sedimentary DNA isolates (15 ng), at least one DNA extraction blank, and
439 one library blank. The libraries were prepared following the established protocol of single stranded DNA
440 library preparation (98) with incubation of second ligation (CL53/CL72) on a thermomixer. Then, all
441 libraries with 50 μL each were frozen at -20°C. These libraries were subjected to qualification, indexing
442 purification, and initial quality controls (99). Four sample libraries underwent agarose gel purification to
443 minimize the impact of adapters on targeted DNA fragments (*SI Appendix, Supplementary Text*).

444 Initially, libraries of 38 sediment samples and nine blanks were equimolarly pooled into four final pools
445 of 10nM each, with a molarity ratio of 10:1 between samples and blanks. They were sequenced on a
446 HiSeq 2500 platform (2 x 125 bp with High-Output V4 mode) and an Illumina NovaSeq 6000 (two pools
447 on 2 x 125 bp and one pool on 2 x 150 bp), respectively. Afterward, we decided to increase the
448 sequencing depth for 16 sedimentary libraries and sequence two additional sediments to obtain better
449 temporal resolution during the mid-Holocene. The 18 sediment samples with four blanks were
450 equimolarly pooled into two pools of 10nM each (with a molarity ratio as above) and sequenced on an
451 Illumina NovaSeq 6000 (2 x 150 bp). The sequencing was performed by *Fasteris* SA (Switzerland) (*SI*
452 *Appendix*, Table S4). Finally, libraries of 40 lake sediments and 12 controls yielded 631.7 GB.

453 **Bioinformatic analyses**

454 We utilized FastQC (v 0.7.11, ref. (100) to assess the quality of the raw reads (2,512,713,391), and
455 then applied clumpify (BBMAP, <https://github.com/BioInfoTools/BBMap/blob/master/sh/clumpify.sh>, v.
456 0.20.1) with default settings, except for the 'dedupe=t' setting, to remove duplicate raw reads.
457 Subsequently, we used Fastp (v. 0.11.9, ref. (101), <https://github.com/OpenGene/fastp>) for adapter
458 trimming and merging of paired-end reads in parallel. The deduplicated reads were trimmed for adapter
459 filter (-a auto) when R1/R2 lacked overlaps, poly G ends (--ploy_g_min_len 10), poly X ends (--
460 ploy_x_min_len 10), quality filter (--qualified_quality_phred 15, --unqualified_percent_limit 40, --
461 n_base_limit 5), length filter (--length_required 30), lower complexity filter (--low_complexity_filter 30).
462 Overlapped reads were merged (-m --merged_out) based on overlapping detection with a minimal
463 overlapped length of 30 bp (overlap_len_require 30), a maximum mismatch limit of 5 (overlap_diff_limit
464 5), and a maximum percentage of mismatch of 20 (overlap_diff_percent_limit 20). Then, the outputs
465 were evaluated by FastQC (v 0.7.11, ref. (100) for quality check.

466 The merged reads (1,724,066,613) were utilized for taxonomic assignment through end-to-end
467 alignment in Bowtie2 (version 2.5.1, ref. (102)) and hereafter using ngsLCA (v. 1.0.5, ref. (49)). We

468 established a taxonomic reference database incorporating all available RefSeq genomes from the NCBI
469 (National Center for Biotechnology Information, downloaded on 14.08.2023). Following the HOLI
470 pipeline (103), this database was constructed using Bowtie2 (version 2.5.1, ref. (102)) with a default
471 setting. The merged reads were aligned against the reference genome databases to identify a maximum
472 of 1000 valid and unique alignments (-k 1000). The resulting possible alignments were sorted and
473 hereafter classified using ngsLCA (v. 1.0.5, ref. (49)) with a minimal identity of 95%.

474 **Ancient DNA (aDNA) authentication and effect of aDNA damage**

475 Short DNA fragmentation and cytosine deamination, indicated by high frequency of C>T substitutions
476 in the 5' and 3' ends (*SI Appendix*, Fig. S2 and Fig. S3), characterize our metagenomic data originating
477 from ancient sources (104). MapDamage2 (v. 2.2.1) was applied on taxonomically classified reads with
478 settings of –rescale and –single-stranded (105). 26 common taxa were authenticated with sufficient
479 reads (*SI Appendix*, Fig. S3) as representations of terrestrial mammalian community (*Bos*, *Cervus*,
480 *Equus*, *Ochotona*, and *Cricetidae*), terrestrial vegetation (Poaceae, Asteraceae, *Carex*, *Rhodiola*,
481 *Saxifraga*, *Potentilla*, *Pedicularis*, *Salix*, and *Salvia*), aquatic vegetation (*Myriophyllum* and
482 *Potamogeton*), fish (Cyprinidae and Salmonidae), and aquatic microbes (*Nannochloropsis*,
483 *Chamaesiphon*, *Leptolyngbya*, *Nostoc*, *Oscillatoria*, *Pseudanabaena*, *Planktothrix*, and *Cyanobium*).

484 We further observed an increase in the frequency of C>T deamination with age (*SI Appendix*, Fig. S4),
485 indicating an effectively closed lake system that prevents DNA from being influenced by re-deposition
486 and environmental variables (detailed discussion in *SI Appendix, Supplementary Text*).

487 **Taxonomic data cleaning and filtering**

488 We obtained 123,786,174 reads assigned to cellular organisms, of which 107,648,162 reads classified
489 to taxa at family or genus level (*SI Appendix*, Fig. S8A). These classified taxa are generally from
490 Bacteria, followed by Eukaryotes and Archaea (*SI Appendix*, Fig. S8B). We detected a few proportions
491 of reads in the blanks (in the range of 0.001 to 0.2%, *SI Appendix*, Table S5), while none of them shared
492 similar taxa composition with the samples (*SI Appendix*, Fig. S9). Niche conservatism is evident in
493 organisms on the Tibetan Plateau, particularly in plants adapted to harsh environmental conditions
494 above 3000 m a.s.l. in our study region (106–108). The observed niche conservatism suggests that
495 species within families and genera tend to preserve ancestral traits, showcasing consistent adaptive
496 strategies for survival in challenging alpine environments over time. To detect the direct associations
497 among taxa above species level, we kept reads belonging to natural seed-bearing plants, macrophytes,
498 fish, and mammals (excluding Hominidae) if their families are recorded above 3000 m a.s.l. in the
499 Tibetan Plateau. If a read is identified at the genus level but cannot be confidently matched to a known
500 occurrence, we assigned it to the family level, assuming that the best-matched genus was absent in the
501 taxonomic reference database. The list of referred families and genera was compiled beforehand (*SI*
502 *Appendix, Supplementary Text*). Meanwhile, we kept Cyanobacteria and Monodopsidaceae (green
503 algae) common in lake. Hereafter, we kept taxa that occur in at least two samples and have a total read
504 count ≥ 5 across all samples (49). Consequently, 94% reads of our targeted taxa were retained (*SI*
505 *Appendix, Fig. S8C*).

506 **Glacier and permafrost simulation**

507 The spatial glacier extent and thickness were simulated using the numerical GC2D ice-flow model with
508 specific settings for our study area, which have been reported in our previous study (45). The modeled
509 glacier dynamics compare well with the changes in clay content ($< 2 \mu\text{m}$) of Lake Naleng sediments
510 that suggest decreasing influences of glaciers after 14.5 ka (94). We further calculated the percentage
511 of glacier extent in the lake catchment (*SI Appendix*, Fig. 10A) and glacier mass from 22–0 ka at 500-
512 year intervals (*SI Appendix*, Fig. 10B). We interpolated permafrost distribution through time (*Appendix*,
513 Fig. 10C, D, and E) from the present-day relationship between permafrost distribution and annual mean
514 air temperature. This present-day relationship was built by a generalized linear model (GLM) and
515 showed a significant P value $< 2\text{e-}16$ (t test with standard errors = 4.03e-05). We compared permafrost
516 distribution at 0 ka with present-day to correct permafrost fields across time and assessed the reliability
517 of the simulated results. We found simulated permafrost dynamics (*SI Appendix*, Fig. S7A) matching
518 well with the relative abundance of those bacteria known from permafrost soils and active layers on the
519 Tibetan Plateau (*SI Appendix*, Fig. S7B and C). Likewise, the simulated results are consistent with

520 regional geological evidence (14). The detailed simulation processes and authentication are provided
521 in *SI Appendix, Supplementary Text*.

522 **Taxonomic composition and ordination analyses**

523 The filtered reads (1,067,557) belonging to 317 taxa were grouped into three count datasets: terrestrial
524 vegetation, terrestrial mammalian, and aquatic ecosystem. There was a higher number of filtered reads
525 in glacial samples than in interglacial samples for the terrestrial and aquatic datasets (*SI Appendix*, Fig.
526 S8C). We calculated the relative abundance to obtain the compositionally equivalent information.

527 The negative binomial distributions (high mean values of read counts also have high variances) were
528 detected in the count datasets (*SI Appendix*, Fig. S11A). To address heterogeneity, the count datasets
529 were normalized using the ‘regularized log’ (rlog) transformation and the variance stabilizing
530 transformation (vst) with default setting in the ‘DESeq2’ package (109). Both methods take sampling
531 depth and composition into account, achieving approximately homoscedastic distributions (*SI Appendix*,
532 Fig. S11B and C). Rlog-based counts, in particular, exhibit smaller standard deviations and were used
533 for RDA and variation partitioning analysis.

534 We linearly interpolated the reconstructed past temperature (110, 111), simulated permafrost extent
535 covering glacier-free lake catchment, and simulated glacier mass to match the temporal resolution of
536 the shotgun data. We used principal component analysis (PCA) on rlog-based terrestrial plant counts
537 using ‘rda(scale = FALSE)’ and extracted PC1 site scores as an indicator of terrestrial vegetation
538 turnover. To estimate the contribution of big herbivores to terrestrial vegetation changes, we extracted
539 the percentage of *Bos* (relative to terrestrial mammalian taxa) recorded by Lake Naleng as an herbivore
540 intensity proxy. *Rumex* and *Sanguisorba* are considered robust indicators of land-use intensity in
541 mountain regions (112–115) because they are commonly found in soils with high levels of nitrogen
542 (*Rumex*) or can withstand grazing and trampling by livestock due to their basal rosette growth habit
543 (*Sanguisorba*). Therefore, we summed up the pollen percentage of both taxa (relative to pollen grains
544 of terrestrial seed-bearing taxa) archived in Lake Naleng as an indicator of land-use intensity.

545 All environmental factors were standardized using the ‘decostand(method = “standardize”)’, ensuring
546 their transformation into variables approximating a normal distribution and achieving dimensional
547 homogeneity (uniform unit variance). Subsequently, three rlog-transformed count datasets (terrestrial
548 vegetation, terrestrial mammalian, and aquatic ecosystem) were separately linked to corresponding
549 environmental variables using the ‘rda’ function. RDA, a linear method, was chosen because the length
550 of the first ordination axis was ≤ 1 standard deviation as indicated by detrended correspondence
551 analysis. Given temperature as a predictor variable for the cryosphere components’ simulation, the
552 multicollinearity tests were implemented on the RDA results using the ‘vif’ function in the ‘car’ package
553 (116) to select the independent environmental drivers (vif score ≤ 3). Then, those independent variables
554 (*SI Appendix*, Table S6 and S7) were used to calculate the unique explanation of variation (= adjusted
555 r^2 value, ref. (117)) with variation partitioning analysis using the ‘varpart’ function.

556 We further verified the consistency of conclusions drawn from the ordination analyses by comparing
557 results based on both the entire set of taxa and a subset of common taxa identified through network
558 analysis (as explained in the next section). Both of them yielded reproducible argumentations for
559 terrestrial vegetation, terrestrial mammalian, and aquatic ecosystem (*SI Appendix*, Table S6, Table S7,
560 and Fig. S12A-C). These analyses were carried out using the ‘vegan’ package (118).

561 **Co-occurrence networks**

562 Multiple taxa may co-occur due to responding to common environments, mediators (e.g., similar
563 abundance changes due to shared consumers), and direct associations (e.g., facilitation) (119). To
564 explore the direct associations, we performed a Gaussian copula graphical model to the count datasets
565 of terrestrial (including vegetation and mammals) and aquatic. This involved using ‘stackedsdm’ to fit
566 the marginal regression model, ‘cord’ for latent factor analysis, and ‘cgr’ for copula graph generation.
567 These functions are available in the ecoCopula package (120). This modeling approach comprises two
568 essential steps: (1) examining conditional dependence relationships (partial correlation obtained from
569 the inverse of the covariance matrix) between pairs of taxa, while considering other correlations across
570 the marginal models; (2) identifying latent drivers and discerning co-occurrence patterns resulting from
571 direct associations from those mediated by environmental factors and mediators (120, 121). Hence, in

572 this study, partial correlations, after accounting for the influence of cryosphere changes, land use, and
573 mediator taxa, serve as representatives of the direct associations among taxa.

574 For each ecosystem, marginal regression models were established both without (H0) and with changes
575 in cryosphere and land use (H1): $H0 = \text{stackedsdm}(Y, \sim 1 + \text{offset}(\log(\text{sizeFactors})))$, data = envi, family
576 = "negative.binomial" and $H1 = \text{stackedsdm}(Y, \sim X + \text{offset}(\log(\text{sizeFactors})))$, data = envi, family =
577 "negative.binomial"). Here, Y represents the raw count data, and X represents the combination of
578 cryosphere and land use. An offset was incorporated to adjust for variations in sampling effort,
579 estimated using 'estimateSizeFactors(type = "ratio")' in the DESeq2 package (109). Dunn-Smyth
580 residuals and normal quantile plots suggest no violation of the assumptions of negative binomial
581 distribution and generalized linear model for both H0 and H1 (SI Appendix, Fig. S13 and Fig. S14).
582 Applying latent factor analysis using the 'cord(nlv = 2, n.samp = 500, seed = 123)' revealed three distinct
583 clusters of sites based on H0, which were not evident based on H1 (SI Appendix, Fig. S6A and B). This
584 suggests that misspecification in H1 has contributed minimally to the identification of direct interactions.

585 Subsequently, graphical models were constructed from H0 using the 'cgr(method = "BIC", seed = 123,
586 n.samp = 500, n.lambda = 100)', while for H1, the specific parameter 'n.lambda' was set to the optimized
587 lambda value obtained from H0\$all_graphs\$lambda.opt. So, both models are comparable. To fit a
588 completely dense graph (one margin to infer the best network), we implemented a thresholding
589 approach, ranging from 0 to 5,000 with a step of 50, to exclude the rare taxa. The upper limit, retaining
590 the top 5% very dominant taxa, is data-dependent and not a universal recommendation. The lowest
591 threshold required to generate the first marginal graph was chosen for subsequent analysis.

592 We assumed that positive associations (e.g., facilitation) among taxa in terrestrial and aquatic
593 ecosystems would be more prevalent during glacial periods compared to interglacial periods, in line
594 with the stress gradient hypothesis (61). To test this assumption, we extracted the positive partial
595 correlations from the best network of H0 and H1 for each ecosystem using 'as_data_frame' in the igraph
596 package (122). The network structure was computed using 'cluster_louvain' with a resolution ranging
597 from 0 to 1 in increments of 0.001. The lowest resolution value was chosen based on two criteria: (1)
598 identical for both H0 and H1, and (2) the modules detected for each network were limited to 2.

599 Taken together, we determined an abundance threshold of 2,450 and a resolution of 0.69 for the
600 terrestrial ecosystem, and an abundance threshold of 50 with a resolution of 0.52 for the aquatic
601 ecosystem. Accordingly, 27 (694,398 reads) out of 274 terrestrial taxa (760,283 reads) and 39 (307,198
602 reads) out 43 aquatic taxa (307,274 reads) were used (referred to as common taxa).

603 We calculated five general network properties, including nodes (taxa), edges (links between taxa),
604 degree centralization, module (community), and Kleinberg's hub centrality scores. The positive links
605 were adjusted as follows: the number of positive links divided by the number of full links of all taxa. We
606 used degree centralization based on the degree of centrality scores of taxa within the module to assess
607 how centralized the network is around a few highly connected taxa. The degree centralization score per
608 module was calculated using 'centr_degree(normalized = TRUE)'. High degree centralization score
609 indicates that a few taxa within the module have significantly higher degrees (associations) than others.
610 The loss of these taxa would significantly impact ecosystem functioning. To assess the taxon
611 importance, we calculated Kleinberg's hub centrality scores using "hub_score(scale = TRUE)" and
612 considered a score of 0.8 as a threshold for being a keystone species. Such hub centrality scores are
613 defined by the principal eigenvector of A^*A^T and rescaled between 0 and 1 by the maximum score (62).

614 All analyses and data visualization were performed under the R environment v.4.2.2 (123), and, unless
615 specified otherwise, default settings were utilized.

616 **Data and code availability**

617 The raw shotgun sequencing data are available in European Nucleotide Archive (ENA,
618 www.ebi.ac.uk/ena/browser/home) with BioProject accession XXX. The source datasets to reproduce
619 the ordination and network analyses are deposited in Dryad Digital Repository with the identifier
620 <https://doi.org/XXX>. The source codes are archived at https://github.com/sisiliu-research/sedaDNA_Naleng.

622 **Acknowledgements**

623 This study was funded by the Impuls- und Vernetzungsfonds – Helmholtz-Gemeinschaft (IVF, Initiative
624 and Networking Fund of the Helmholtz Association to U.H.), Deutsche Forschungsgemeinschaft (DFG,
625 German Research Foundation, grants 410561986 to S.K., Mi 730/1-1,2 to S.M.), and China Scholarship
626 Council (grant 201606180048 to S.L.).

627 **References**

- 628 1. C. Körner, “Mountain biodiversity, its causes and function: an overview” in *Mountain Biodiversity*,
629 (Routledge, 2019), pp. 3–20.
- 630 2. M. Stibal, *et al.*, Glacial ecosystems are essential to understanding biodiversity responses to
631 glacier retreat. *Nat. Ecol. Evol.* **4**, 686–687 (2020).
- 632 3. X. Jin, *et al.*, Impacts of climate-induced permafrost degradation on vegetation: A review. *Adv.*
633 *Clim. Change Res.* **12**, 29–47 (2021).
- 634 4. M. Li, *et al.*, Climate variability rather than livestock grazing dominates changes in alpine
635 grassland productivity across Tibet. *Front. Ecol. Evol.* **9**, 631024 (2021).
- 636 5. Mountain Research Initiative EDW Working Group, Elevation-dependent warming in mountain
637 regions of the world. *Nat. Clim. Change* **5**, 424–430 (2015).
- 638 6. D. Zou, *et al.*, A new map of permafrost distribution on the Tibetan Plateau. *The Cryosphere* **11**,
639 2527–2542 (2017).
- 640 7. M. Yang, X. Wang, G. Pang, G. Wan, Z. Liu, The Tibetan Plateau cryosphere: Observations and
641 model simulations for current status and recent changes. *Earth-Sci. Rev.* **190**, 353–369 (2019).
- 642 8. B. Verrall, C. M. Pickering, Alpine vegetation in the context of climate change: A global review of
643 past research and future directions. *Sci. Total Environ.* **748**, 141344 (2020).
- 644 9. D. Rhode, *et al.*, Epipaleolithic/early Neolithic settlements at Qinghai Lake, western China. *J.*
645 *Archaeol. Sci.* **34**, 600–612 (2007).
- 646 10. Z. Tang, Z. Wang, C. Zheng, J. Fang, Biodiversity in China’s mountains. *Front. Ecol. Environ.* **4**,
647 347–352 (2006).
- 648 11. D. R. Rounce, R. Hock, D. E. Shean, Glacier mass change in high mountain Asia through 2100
649 using the open-source Python Glacier Evolution Model (PyGEM). *Front. Earth Sci.* **7**, 331 (2020).
- 650 12. G. Zhang, *et al.*, Qinghai-Tibet Plateau permafrost at risk in the late 21st century. *Earth's Future*
651 **10**, e2022EF002652 (2022).
- 652 13. S. Zhou, J. Li, J. Zhao, J. Wang, J. Zheng, “Chapter 70 - Quaternary glaciations: extent and
653 chronology in China” in *Developments in Quaternary Sciences*, Quaternary Glaciations - Extent
654 and Chronology., J. Ehlers, P. L. Gibbard, P. D. Hughes, Eds. (Elsevier, 2011), pp. 981–1002.
- 655 14. H. Jin, *et al.*, Quaternary permafrost in China: framework and discussions. *Quaternary* **3**, 32
656 (2020).
- 657 15. L. Tang, C. Shen, H. Lu, C. Li, Q. Ma, Fifty years of Quaternary palynology in the Tibetan Plateau.
658 *Sci. China Earth Sci.* **64**, 1825–1843 (2021).
- 659 16. S. A. Zimov, *et al.*, Steppe-tundra transition: a herbivore-driven biome shift at the end of the
660 Pleistocene. *Am. Nat.* **146**, 765–794 (1995).

- 661 17. S. A. Zimov, N. S. Zimov, A. N. Tikhonov, F. S. Chapin, Mammoth steppe: a high-productivity
662 phenomenon. *Quat. Sci. Rev.* **57**, 26–45 (2012).
- 663 18. Y. Malhi, *et al.*, Megafauna and ecosystem function from the Pleistocene to the Anthropocene.
664 *Proc. Natl. Acad. Sci.* **113**, 838–846 (2016).
- 665 19. Z. Wang, *et al.*, Phylogeographical analyses of domestic and wild yaks based on mitochondrial
666 DNA: new data and reappraisal. *J. Biogeogr.* **37**, 2332–2344 (2010).
- 667 20. M. Macias-Fauria, P. Jepson, N. Zimov, Y. Malhi, Pleistocene Arctic megafaunal ecological
668 engineering as a natural climate solution? *Philos. Trans. R. Soc. B Biol. Sci.* **375**, 20190122 (2020).
- 669 21. X. L. Zhang, *et al.*, The earliest human occupation of the high-altitude Tibetan Plateau 40
670 thousand to 30 thousand years ago. *Science* **362**, 1049–1051 (2018).
- 671 22. F. H. Chen, *et al.*, Agriculture facilitated permanent human occupation of the Tibetan Plateau after
672 3600 B.P. *Science* **347**, 248–250 (2015).
- 673 23. Q. Qiu, *et al.*, Yak whole-genome resequencing reveals domestication signatures and prehistoric
674 population expansions. *Nat. Commun.* **6**, 10283 (2015).
- 675 24. F. Schlütz, F. Lehmkühl, Holocene climatic change and the nomadic Anthropocene in Eastern
676 Tibet: palynological and geomorphological results from the Nianbaoyeze Mountains. *Quat. Sci.*
677 *Rev.* **28**, 1449–1471 (2009).
- 678 25. A. Kramer, U. Herzschuh, S. Mischke, C. Zhang, Holocene treeline shifts and monsoon variability
679 in the Hengduan Mountains (southeastern Tibetan Plateau), implications from palynological
680 investigations. *Palaeogeogr. Palaeoclimatol. Palaeoecol.* **286**, 23–41 (2010).
- 681 26. G. Miehe, *et al.*, The Kobresia pygmaea ecosystem of the Tibetan highlands – Origin, functioning
682 and degradation of the world's largest pastoral alpine ecosystem: Kobresia pastures of Tibet. *Sci.*
683 *Total Environ.* **648**, 754–771 (2019).
- 684 27. X. Xiao, A. Yao, A. Hillman, J. Shen, S. G. Haberle, Vegetation, climate and human impact since
685 20 ka in central Yunnan Province based on high-resolution pollen and charcoal records from
686 Dianchi, southwestern China. *Quat. Sci. Rev.* **236**, 106297 (2020).
- 687 28. G. Miehe, *et al.*, Föhn, fire and grazing in Southern Tibet? A 20,000-year multi-proxy record in an
688 alpine ecotonal ecosystem. *Quat. Sci. Rev.* **256**, 106817 (2021).
- 689 29. L. W. Lehnert, K. Wesche, K. Trachte, C. Reudenbach, J. Bendix, Climate variability rather than
690 overstocking causes recent large scale cover changes of Tibetan pastures. *Sci. Rep.* **6**, 24367
691 (2016).
- 692 30. F. Tian, *et al.*, Palynological evidence for the temporal stability of the plant community in the
693 Yellow River Source Area over the last 7,400 years. *Veg. Hist. Archaeobot.* (2022)
694 <https://doi.org/10.1007/s00334-022-00870-5> (April 12, 2022).
- 695 31. K. Bauer, Y. Nyima, Laws and Regulations Impacting the Enclosure Movement on the Tibetan
696 Plateau of China. *HIMALAYA J. Assoc. Nepal Himal. Stud.* **30** (2011).
- 697 32. B. Aichner, U. Herzschuh, H. Wilkes, A. Vieth, J. Böhner, δ D values of n-alkanes in Tibetan lake
698 sediments and aquatic macrophytes – A surface sediment study and application to a 16ka record
699 from Lake Koucha. *Org. Geochem.* **41**, 779–790 (2010).
- 700 33. U. Herzschuh, S. Mischke, H. Meyer, B. Plessen, C. Zhang, Lake nutrient variability inferred from
701 elemental (C, N, S) and isotopic (δ 13C, δ 15N) analyses of aquatic plant macrofossils. *Quat. Sci.*
702 *Rev.* **29**, 2161–2172 (2010).

- 703 34. Z. Baiping, C. Xiaodong, L. Baolin, Y. Yonghui, Biodiversity and conservation in the Tibetan
704 Plateau. *J. Geogr. Sci.* **12**, 135–143 (2002).
- 705 35. U. Herzschuh, *et al.*, A late Quaternary lake record from the Qilian Mountains (NW China):
706 evolution of the primary production and the water depth reconstructed from macrofossil, pollen,
707 biomarker, and isotope data. *Glob. Planet. Change* **46**, 361–379 (2005).
- 708 36. J. Saini, *et al.*, Climate variability in the past ~19,000 yr in NE Tibetan Plateau inferred from
709 biomarker and stable isotope records of Lake Dongji Cona. *Quat. Sci. Rev.* **157**, 129–140 (2017).
- 710 37. B. Aichner, *et al.*, Asynchronous responses of aquatic ecosystems to hydroclimatic forcing on the
711 Tibetan Plateau. *Commun. Earth Environ.* **3**, 1–11 (2022).
- 712 38. S. Huo, H. Zhang, J. Wang, J. Chen, F. Wu, Temperature and precipitation dominates millennium
713 changes of eukaryotic algal communities in Lake Yamzhog Yumco, Southern Tibetan Plateau.
714 *Sci. Total Environ.* **829**, 154636 (2022).
- 715 39. A. I. T. Tulloch, *et al.*, Dynamic species co-occurrence networks require dynamic biodiversity
716 surrogates. *Ecography* **39**, 1185–1196 (2016).
- 717 40. A. D. Muscente, *et al.*, Quantifying ecological impacts of mass extinctions with network analysis
718 of fossil communities. *Proc. Natl. Acad. Sci.* **115**, 5217–5222 (2018).
- 719 41. M. D. Bertness, R. Callaway, Positive interactions in communities. *Trends Ecol. Evol.* **9**, 191–193
720 (1994).
- 721 42. Y. Wang, J. Sun, B. Liu, J. Wang, T. Zeng, Cushion plants as critical pioneers and engineers in
722 alpine ecosystems across the Tibetan Plateau. *Ecol. Evol.* **11**, 11554–11558 (2021).
- 723 43. Y. Zhang, *et al.*, Diversity patterns of cushion plants on the Qinghai-Tibet Plateau: A basic study
724 for future conservation efforts on alpine ecosystems. *Plant Divers.* **44**, 231–242 (2022).
- 725 44. F. Anthelme, L. A. Cavieres, O. Dangles, Facilitation among plants in alpine environments in the
726 face of climate change. *Front. Plant Sci.* **5**, 387 (2014).
- 727 45. S. Liu, *et al.*, Sedimentary ancient DNA reveals a threat of warming-induced alpine habitat loss to
728 Tibetan Plateau plant diversity. *Nat. Commun.* **12**, 2995 (2021).
- 729 46. H. J. B. Birks, A. F. Lotter, S. Juggins, J. P. Smol, Eds., *Tracking Environmental Change Using
730 Lake Sediments* (Springer Netherlands, 2012), pp. 4–5.
- 731 47. W. Jia, *et al.*, Sedimentary ancient DNA reveals past ecosystem and biodiversity changes on the
732 Tibetan Plateau: Overview and prospects. *Quat. Sci. Rev.* **293**, 107703 (2022).
- 733 48. K. H. Kjær, *et al.*, A 2-million-year-old ecosystem in Greenland uncovered by environmental DNA.
734 *Nature* **612**, 283–291 (2022).
- 735 49. Y. Wang, T. S. Korneliussen, L. E. Holman, A. Manica, M. W. Pedersen, ngsLCA—A toolkit for
736 fast and flexible lowest common ancestor inference and taxonomic profiling of metagenomic data.
737 *Methods Ecol. Evol.* **13**, 2699–2708 (2022).
- 738 50. A. Kramer, U. Herzschuh, S. Mischke, C. Zhang, Late glacial vegetation and climate oscillations
739 on the southeastern Tibetan Plateau inferred from the Lake Naleng pollen profile. *Quat. Res.* **73**,
740 324–335 (2010).
- 741 51. B. Kang, *et al.*, Mapping China's freshwater fishes: diversity and biogeography. *Fish Fish.* **15**,
742 209–230 (2014).

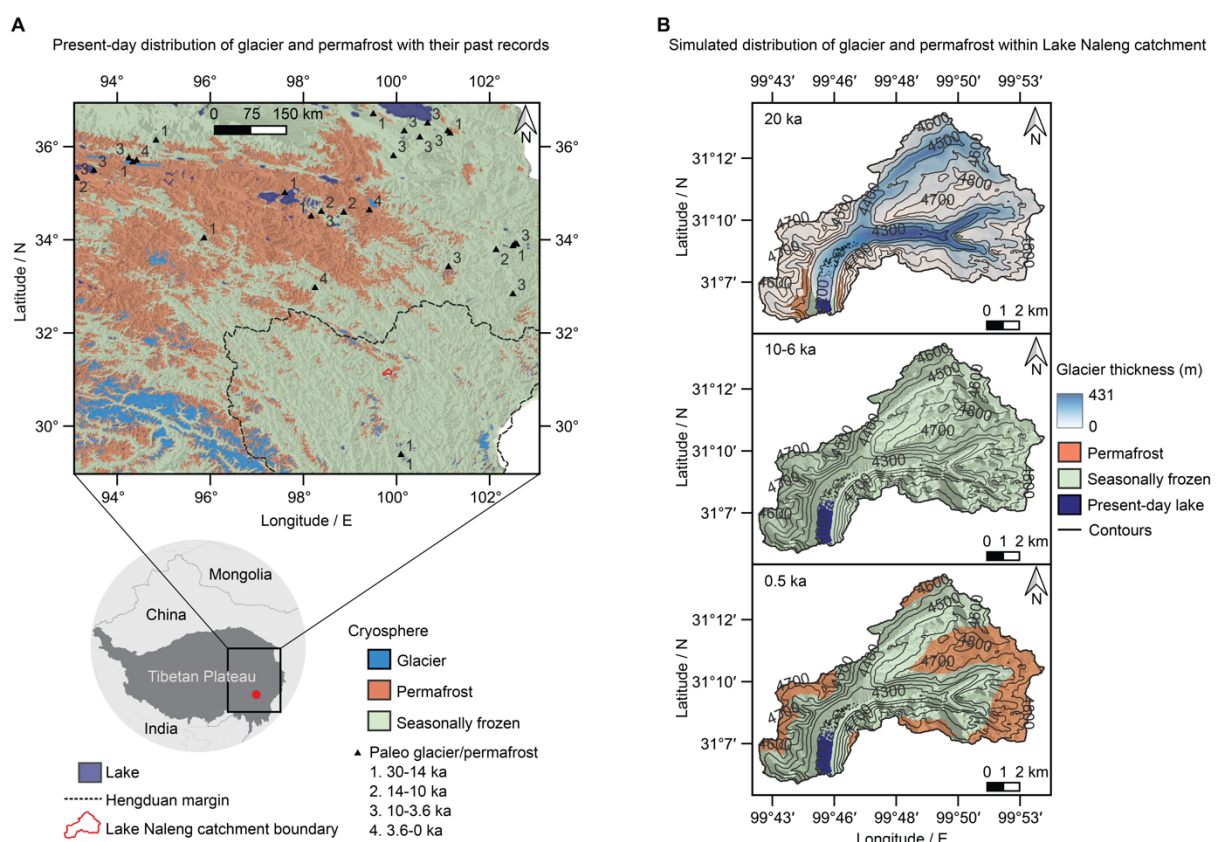
- 743 52. L. Zhang, *et al.*, The neglected otters in China: Distribution change in the past 400 years and
744 current conservation status. *Biol. Conserv.* **228**, 259–267 (2018).
- 745 53. Y. Lammers, P. D. Heintzman, I. G. Alsos, Environmental palaeogenomic reconstruction of an Ice
746 Age algal population. *Commun. Biol.* **4**, 1–11 (2021).
- 747 54. J. Huisman, *et al.*, Cyanobacterial blooms. *Nat. Rev. Microbiol.* **16**, 471–483 (2018).
- 748 55. J. Courtin, *et al.*, Pleistocene glacial and interglacial ecosystems inferred from ancient DNA
749 analyses of permafrost sediments from Batagay megaslump, East Siberia. *Environ. DNA* **4**, 1265–
750 1283 (2022).
- 751 56. M. W. Pedersen, *et al.*, Postglacial viability and colonization in North America's ice-free corridor.
752 *Nature* **537**, 45–49 (2016).
- 753 57. L. Parducci, *et al.*, Shotgun environmental DNA, pollen, and macrofossil analysis of Lateglacial
754 lake sediments from southern Sweden. *Front. Ecol. Evol.* **7**, 189 (2019).
- 755 58. Y. Wang, *et al.*, Late Quaternary dynamics of Arctic biota from ancient environmental genomics.
756 *Nature* **600**, 86–92 (2021).
- 757 59. K. Li, *et al.*, Plant sedimentary DNA as a proxy for vegetation reconstruction in eastern and
758 northern Asia. *Ecol. Indic.* **132**, 108303 (2021).
- 759 60. Z. Wende, *et al.*, Reconstruction of cultivated land in the northeast margin of Qinghai–Tibetan
760 Plateau and anthropogenic impacts on palaeo-environment during the mid-Holocene. *Front. Earth
761 Sci.* **9** (2021).
- 762 61. A. E. Adams, E. M. Besozzi, G. Shahrokhi, M. A. Patten, A case for associational resistance:
763 Apparent support for the stress gradient hypothesis varies with study system. *Ecol. Lett.* **25**, 202–
764 217 (2022).
- 765 62. J. M. Kleinberg, Authoritative sources in a hyperlinked environment. *J. ACM* **46**, 604–632 (1999).
- 766 63. G. Yang, *et al.*, Multiple anthropogenic pressures eliminate the effects of soil microbial diversity
767 on ecosystem functions in experimental microcosms. *Nat. Commun.* **13**, 4260 (2022).
- 768 64. C. V. Robinson, T. M. Porter, V. C. Maitland, M. T. G. Wright, M. Hajibabaei, Multi-marker
769 metabarcoding resolves subtle variations in freshwater condition: Bioindicators, ecological traits,
770 and trophic interactions. *Ecol. Indic.* **145**, 109603 (2022).
- 771 65. G. Bao, *et al.*, Effects of the hemiparasitic plant *Pedicularis kansuensis* on plant community
772 structure in a degraded grassland. *Ecol. Res.* **30**, 507–515 (2015).
- 773 66. L. A. Cavieres, E. I. Badano, Do facilitative interactions increase species richness at the entire
774 community level? *J. Ecol.* **97**, 1181–1191 (2009).
- 775 67. J. Ebersbach, J. Schnitzler, A. Favre, A. N. Muellner-Riehl, Evolutionary radiations in the species-
776 rich mountain genus *Saxifraga* L. *BMC Evol. Biol.* **17**, 119 (2017).
- 777 68. X. Jing, *et al.*, The adaptive strategies of yaks to live in the Asian highlands. *Anim. Nutr.* **9**, 249–
778 258 (2022).
- 779 69. A. Kramer, U. Herzschuh, S. Mischke, C. Zhang, Late Quaternary environmental history of the
780 south-eastern Tibetan Plateau inferred from the Lake Naleng non-pollen palynomorph record.
781 *Veg. Hist. Archaeobotany* **19**, 453–468 (2010).
- 782 70. N. Guo, *et al.*, Seasonal dynamics of diet–gut microbiota interaction in adaptation of yaks to life
783 at high altitude. *Npj Biofilms Microbiomes* **7**, 1–11 (2021).

- 784 71. S. K. Basumatary, *et al.*, Coprophilous and non-coprophilous fungal spores of *Bos mutus* modern
785 dung from the Indian Himalaya: Implications to temperate paleoherbivory and paleoecological
786 analysis. *Rev. Palaeobot. Palynol.* **277**, 104208 (2020).
- 787 72. E. Willerslev, *et al.*, Fifty thousand years of Arctic vegetation and megafaunal diet. *Nature* **506**,
788 47–51 (2014).
- 789 73. I. C. Barrio, D. S. Hik, C. G. Bueno, J. F. Cahill, Extending the stress-gradient hypothesis – is
790 competition among animals less common in harsh environments? *Oikos* **122**, 516–523 (2013).
- 791 74. T. J. Murchie, *et al.*, Collapse of the mammoth-steppe in central Yukon as revealed by ancient
792 environmental DNA. *Nat. Commun.* **12**, 7120 (2021).
- 793 75. E. Politti, W. Bertoldi, A. Gurnell, A. Henshaw, Feedbacks between the riparian Salicaceae and
794 hydrogeomorphic processes: A quantitative review. *Earth-Sci. Rev.* **176**, 147–165 (2018).
- 795 76. C. Yang, T. Yan, Y. Sun, F. Hou, Shrub cover impacts on yak growth performance and
796 herbaceous forage quality on the Qinghai-Tibet Plateau, China. *Rangel. Ecol. Manag.* **75**, 9–16
797 (2021).
- 798 77. A. J. Monteath, B. V. Gaglioti, M. E. Edwards, D. Froese, Late Pleistocene shrub expansion
799 preceded megafauna turnover and extinctions in eastern Beringia. *Proc. Natl. Acad. Sci.* **118**,
800 e2107977118 (2021).
- 801 78. J. d'Alpoim Guedes, Rethinking the spread of agriculture to the Tibetan Plateau. *The Holocene*
802 **25**, 1498–1510 (2015).
- 803 79. P. Rozwalak, *et al.*, Cryoconite-From minerals and organic matter to bioengineered sediments on
804 glacier's surfaces. *Sci. Total Environ.* **807**, 150874 (2022).
- 805 80. K. Liu, *et al.*, Bacterial community changes in a glacial-fed Tibetan lake are correlated with glacial
806 melting. *Sci. Total Environ.* **651**, 2059–2067 (2019).
- 807 81. K. Liu, *et al.*, Fate of glacier surface snow-originating bacteria in the glacier-fed hydrologic
808 continuums. *Environ. Microbiol.* **23**, 6450–6462 (2021).
- 809 82. J. Kleinteich, K. Hanselmann, F. Hildebrand, A. Kappler, C. Zarfl, Glacier melt-down changes
810 habitat characteristics and unique microbial community composition and physiology in alpine lake
811 sediments. *FEMS Microbiol. Ecol.* **98**, fiac075 (2022).
- 812 83. C. Fournier, E. Riehle, D. R. Dietrich, D. Schleheck, Is toxin-producing *planktothrix* sp. an
813 emerging species in Lake Constance? *Toxins* **13**, 666 (2021).
- 814 84. S. P. Hammarlund, W. R. Harcombe, Refining the stress gradient hypothesis in a microbial
815 community. *Proc. Natl. Acad. Sci. U. S. A.* **116**, 15760–15762 (2019).
- 816 85. E. Hesse, *et al.*, Stress causes interspecific facilitation within a compost community. *Ecol. Lett.*
817 **24**, 2169–2177 (2021).
- 818 86. K. R. Stoof-Leichsenring, *et al.*, Sedimentary DNA identifies modern and past macrophyte
819 diversity and its environmental drivers in high-latitude and high-elevation lakes in Siberia and
820 China. *Limnol. Oceanogr.* **67**, 1126–1141 (2022).
- 821 87. J. Tao, *et al.*, Strong evidence for changing fish reproductive phenology under climate warming
822 on the Tibetan Plateau. *Glob. Change Biol.* **24**, 2093–2104 (2018).
- 823 88. C. Liu, L. Comte, W. Xian, Y. Chen, J. D. Olden, Current and projected future risks of freshwater
824 fish invasions in China. *Ecography* **42**, 2074–2083 (2019).

- 825 89. C. Ayres, P. García, Features of the predation of the Eurasian otter upon toads in north-western
826 Spain. *Mamm. Biol.* **76**, 90–92 (2011).
- 827 90. S. Nakai, S. Yamada, M. Hosomi, Anti-cyanobacterial fatty acids released from *Myriophyllum*
828 *spicatum*. *Hydrobiologia* **543**, 71–78 (2005).
- 829 91. Z. A. Mohamed, Macrophytes-cyanobacteria allelopathic interactions and their implications for
830 water resources management—A review. *Limnologica* **63**, 122–132 (2017).
- 831 92. L. Randsalu-Wendrup, D. J. Conley, J. Carstensen, S. C. Fritz, Paleolimnological records of
832 regime shifts in lakes in response to climate change and anthropogenic activities. *J. Paleolimnol.*
833 **56**, 1–14 (2016).
- 834 93. K. A. Hopping, S. M. Chignell, E. F. Lambin, The demise of caterpillar fungus in the Himalayan
835 region due to climate change and overharvesting. *Proc. Natl. Acad. Sci.* **115**, 11489–11494 (2018).
- 836 94. S. Opitz, C. Zhang, U. Herzschuh, S. Mischke, Climate variability on the south-eastern Tibetan
837 Plateau since the Lateglacial based on a multiproxy approach from Lake Naleng – comparing
838 pollen and non-pollen signals. *Quat. Sci. Rev.* **115**, 112–122 (2015).
- 839 95. S. Strasky, *et al.*, Late Glacial ice advances in southeast Tibet. *J. Asian Earth Sci.* **34**, 458–465
840 (2009).
- 841 96. F. Chen, *et al.*, Climate change, vegetation history, and landscape responses on the Tibetan
842 Plateau during the Holocene: A comprehensive review. *Quat. Sci. Rev.* **243**, 106444 (2020).
- 843 97. P. A. Meyers, Preservation of elemental and isotopic source identification of sedimentary organic
844 matter. *Chem. Geol.* **114**, 289–302 (1994).
- 845 98. M. T. Gansauge, *et al.*, Single-stranded DNA library preparation from highly degraded DNA using
846 T4 DNA ligase. *Nucleic Acids Res.* **45**, e79–e79 (2017).
- 847 99. M. T. Gansauge, M. Meyer, Single-stranded DNA library preparation for the sequencing of ancient
848 or damaged DNA. *Nat. Protoc.* **8**, 737–748 (2013).
- 849 100. S. Andrews, FastQC: a quality control tool for high throughput sequence data [online] (2010).
- 850 101. S. Chen, Y. Zhou, Y. Chen, J. Gu, fastp: an ultra-fast all-in-one FASTQ preprocessor.
851 *Bioinformatics* **34**, i884–i890 (2018).
- 852 102. B. Langmead, S. L. Salzberg, Fast gapped-read alignment with Bowtie 2. *Nat. Methods* **9**, 357–
853 359 (2012).
- 854 103. K. H. Kjær, *et al.*, A 2-million-year-old ecosystem in Greenland uncovered by environmental DNA.
855 *Nature* **612**, 283–291 (2022).
- 856 104. J. Dabney, M. Meyer, S. Paabo, Ancient DNA Damage. *Cold Spring Harb. Perspect. Biol.* **5**,
857 a012567–a012567 (2013).
- 858 105. H. Jónsson, A. Ginolhac, M. Schubert, P. L. F. Johnson, L. Orlando, mapDamage2.0: fast
859 approximate Bayesian estimates of ancient DNA damage parameters. *Bioinformatics* **29**, 1682–
860 1684 (2013).
- 861 106. J. He, *et al.*, Joint effects of environmental filtering and dispersal limitation on the species
862 assemblage of the Tibetan Plateau. *J. Biogeogr.* **49**, 640–653 (2022).
- 863 107. X. H. Li, X. X. Zhu, Y. Niu, H. Sun, Phylogenetic clustering and overdispersion for alpine plants
864 along elevational gradient in the Hengduan Mountains Region, southwest China: Phylogenetic
865 structure along elevational gradient. *J. Syst. Evol.* **52**, 280–288 (2014).

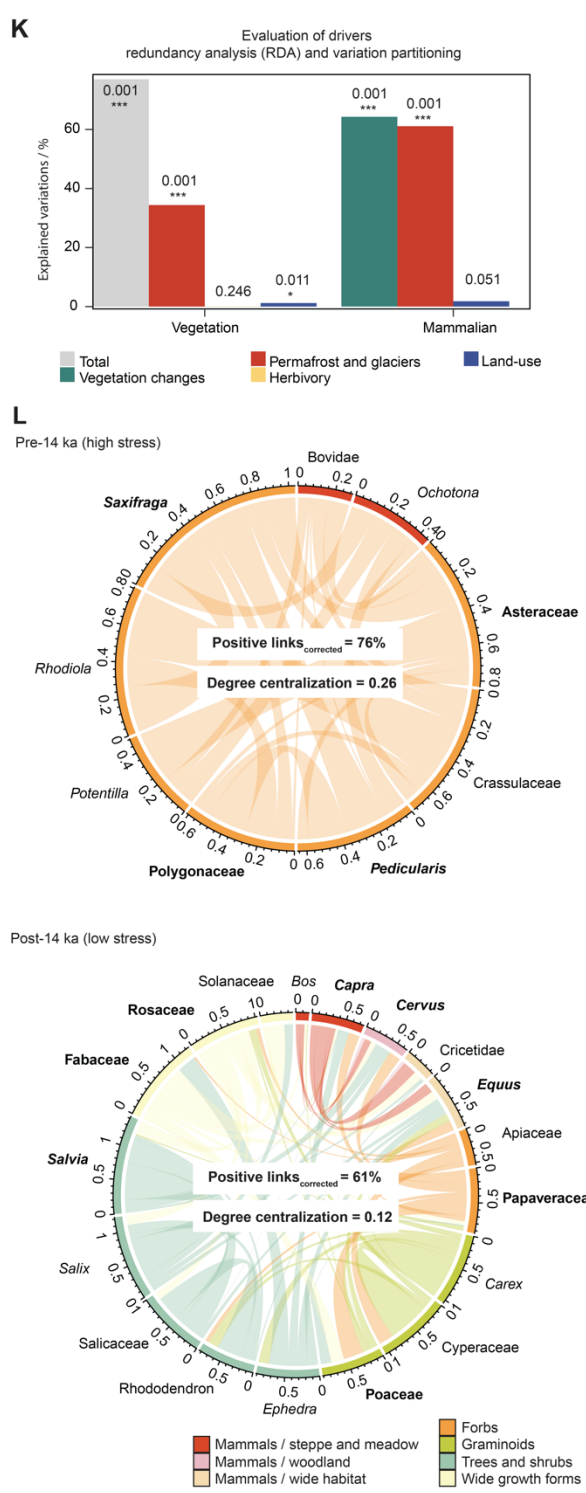
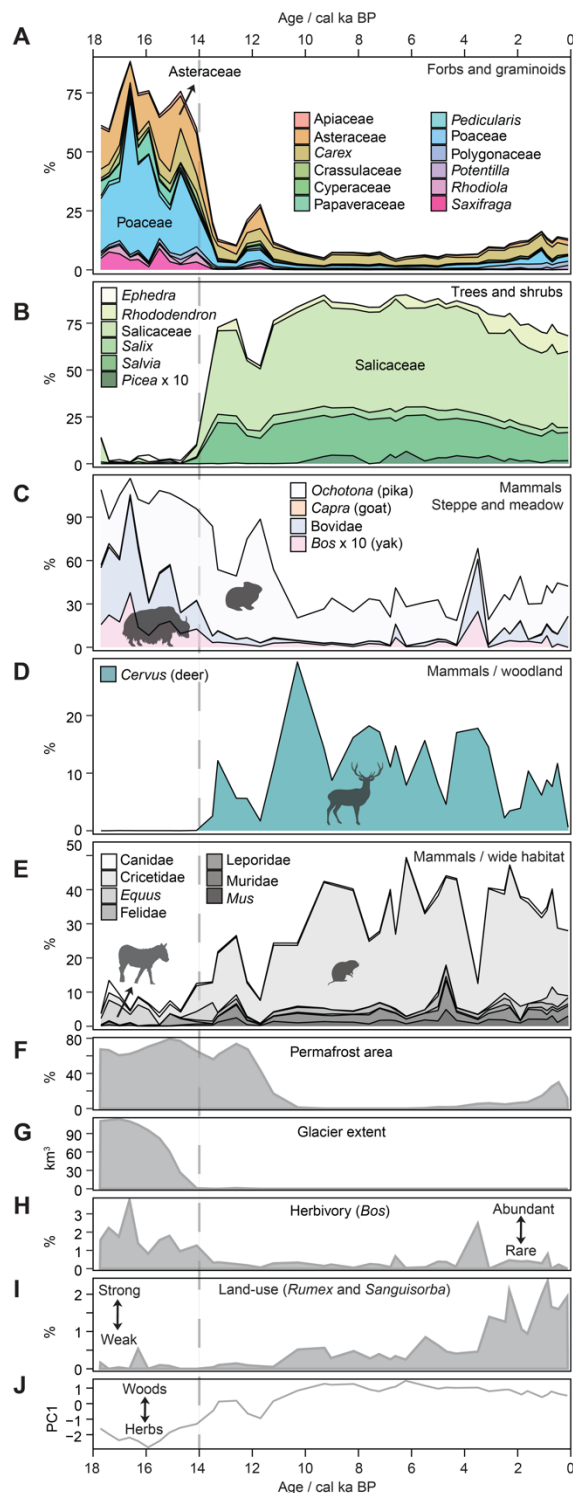
- 866 108. J. Xu, *et al.*, Using phylogeny and functional traits for assessing community assembly along
867 environmental gradients: A deterministic process driven by elevation. *Ecol. Evol.* **7**, 5056–5069
868 (2017).
- 869 109. M. I. Love, W. Huber, S. Anders, Moderated estimation of fold change and dispersion for RNA-
870 seq data with DESeq2. *Genome Biol.* **15**, 550 (2014).
- 871 110. J. D. Shakun, *et al.*, Global warming preceded by increasing carbon dioxide concentrations during
872 the last deglaciation. *Nature* **484**, 49–54 (2012).
- 873 111. S. A. Marcott, J. D. Shakun, P. U. Clark, A. C. Mix, A reconstruction of regional and global
874 temperature for the past 11,300 years. *Science* **339**, 1198–1201 (2013).
- 875 112. Z. Xie, *et al.*, Identifying response groups of soil nitrifiers and denitrifiers to grazing and associated
876 soil environmental drivers in Tibetan alpine meadows. *Soil Biol. Biochem.* **77**, 89–99 (2014).
- 877 113. M. Court-Picon, A. Buttler, J. L. de Beaulieu, Modern pollen/vegetation/land-use relationships in
878 mountain environments: an example from the Champsaur valley (French Alps). *Veg. Hist. Archaeobot.* **15**, 151–168 (2006).
- 880 114. M. Ma, J. I. Walck, Z. Ma, L. Wang, G. Du, Grazing disturbance increases transient but decreases
881 persistent soil seed bank. *Ecol. Appl.* **28**, 1020–1031 (2018).
- 882 115. C. M. Paurer, J. Isselstein, T. Braunbeck, M. K. Schneider, Influence of Highland and production-
883 oriented cattle breeds on pasture vegetation: A pairwise assessment across broad environmental
884 gradients. *Agric. Ecosyst. Environ.* **284**, 106585 (2019).
- 885 116. J. Fox, S. Weisberg, J. Fox, *An R companion to applied regression*, 2nd ed (SAGE Publications,
886 2011).
- 887 117. P. R. Peres-Neto, P. Legendre, S. Dray, D. Borcard, Variation partitioning of species data matrices:
888 estimation and comparison of fractions. *Ecology* **87**, 2614–2625 (2006).
- 889 118. J. Oksanen, *et al.*, vegan: Community Ecology Package (2019).
- 890 119. F. Valladares, C. C. Bastias, O. Godoy, E. Granda, A. Escudero, Species coexistence in a
891 changing world. *Front. Plant Sci.* **6** (2015).
- 892 120. G. C. Popovic, D. I. Warton, F. J. Thomson, F. K. C. Hui, A. T. Moles, Untangling direct species
893 associations from indirect mediator species effects with graphical models. *Methods Ecol. Evol.* **10**,
894 1571–1583 (2019).
- 895 121. G. C. Popovic, F. K. C. Hui, D. I. Warton, A general algorithm for covariance modeling of discrete
896 data. *J. Multivar. Anal.* **165**, 86–100 (2018).
- 897 122. G. Csardi, T. Nepusz, The igraph software package for complex network research. *InterJournal
898 Complex Syst.* **1695**, 1–9 (2006).
- 899 123. R Core Team, R: A Language and Environment for Statistical Computing (2021).
- 900

901 **Figures**

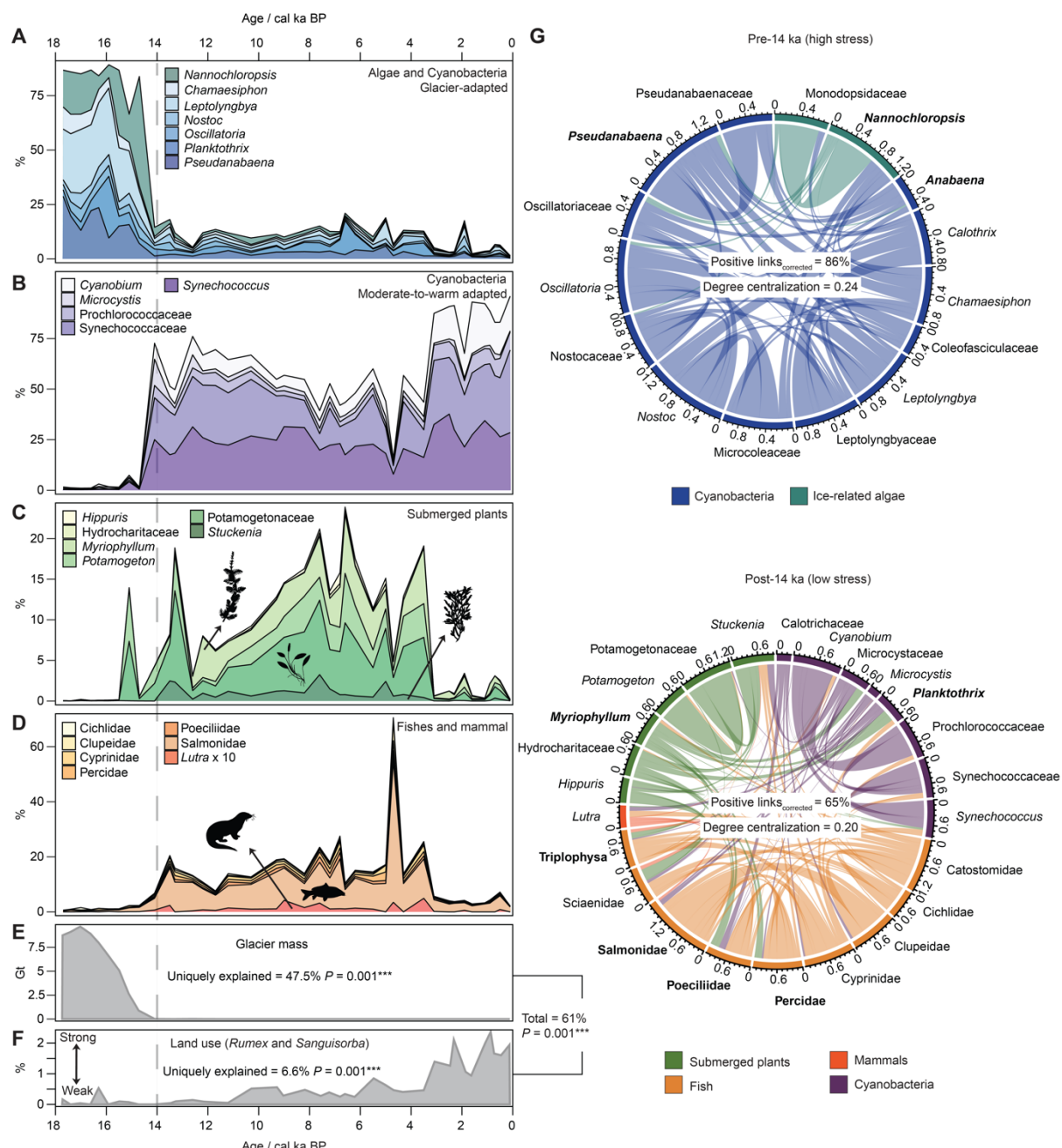


902

903 **Fig. 1 Lake Naleng, located on the southeast Tibetan Plateau (Hengduan Mountains), a global**
904 **biodiversity hotspot, is influenced by the past and modern cryosphere.** (A) Modern glacier and
905 permafrost distribution (6) with their past records (14) indicate a southeastward advance of the
906 cryosphere until 14 ka and a northeastward retreat afterward. (B) The simulated glaciers and permafrost
907 distribution (Materials and Methods, SI Appendix, Fig. S1) indicate that Lake Naleng with its catchment
908 was strongly influenced by the cryosphere during the late glacial period, while without impact during the
909 early-to-mid Holocene. Permafrost, but not glaciers, recovered during the late Holocene, mostly in the
910 highlands in the east of the lake catchment.



912 **Fig. 2 Long-term trends in shotgun-based (metagenomics) main terrestrial taxa recorded in Lake**
913 **Naleng compared with temporal changes of environmental factors.** (A-B) The shotgun-based
914 relative abundance of the common terrestrial vegetation community indicates a transition from steppe-
915 meadow pre-14 ka to woodland post-14 ka. (C-E) The shotgun-based relative abundance of the
916 common terrestrial mammalian community shows a loss of wild megafauna since 14 ka. (F) The
917 percentages of simulated glacier-free permafrost extent within the lake catchment (Methods and
918 Materials). (G) The modeled glacier extent within the lake catchment (45). (H) The shotgun-based
919 relative abundance of *Bos* relative to mammalian community as a signal of herbivory. (I) The
920 percentages of *Rumex* and *Sanguisorba* relative to the pollen grains of terrestrial seed-bearing plants
921 recorded in Lake Naleng as an indicator of intensity of land use (25, 50). (J) The principal curve of the
922 terrestrial vegetation changes shows a transition from steppe-meadow with dominant herbs and
923 graminoids in the pre-14 ka period to woodland dominated by willow shrubs and trees. (K) Evaluation
924 of drivers based on redundancy analysis (RDA) and variation partitioning shows that cryosphere
925 (permafrost and glacier extent) explains the highest unique portion of variation in the vegetation and
926 mammalian communities. These results refute the perspective of top-down control by large herbivores
927 in the ecosystem and significant land use in the creation of the modern alpine ecosystem on the Tibetan
928 Plateau. Explained variations are represented by percentages of adjusted r^2 values, obtained from RDA
929 for joint explanation and variation partitioning for unique explanation. (L) Weighted network analyses
930 based on positive partial correlations classify two modules, characterized by common taxa in the pre-
931 14 ka (glacial) period with a high percentage of positive links and the post-14 ka (interglacial) period
932 with a low percentage of positive links. Such structures support the stress-gradient hypothesis that
933 positive interactions among organisms occur more frequently in a high stress environment. Further,
934 more taxa connected via mediators developed in the cold phase suggesting a higher degree of
935 centralization. Taxa with Kleinberg's hub centrality score ≥ 0.8 (normalized score into an arbitrary range
936 of 0–1 by taking maximum score into account) are considered keystone taxa and marked in bold. The
937 percentage of positive links has been adjusted to the number of taxa. The chord thickness represents
938 the positive partial correlation. The proportions of *Picea* and *Bos* are aggregated 10 times for better
939 visibility.



941 **Fig. 3 Long-term changes in shotgun-based (metagenomics) aquatic communities recorded in**
942 **Lake Naleng compared with temporal changes of environmental factors.** (A-D) Changes in the
943 relative abundance of the common taxa indicate a shift from abundant glacier-adapted microbes (algae
944 and cyanobacteria) in the pre-14 ka period to non-glacier-adapted picocyanobacteria, submerged
945 plants, fish, and fish-eating otters until 3.6 ka, followed by overabundance of picocyanobacteria in the
946 post-3.6 ka interval. (E-F) Evaluation of environmental factors suggests a high contribution of glacier
947 mass on aquatic community composition changes. Explained variations are represented by adjusted r^2
948 values, obtained from RDA for joint explanation and variation partitioning for unique explanation. (G)
949 Weighted network analyses based on positive partial correlations classify two modules, characterized
950 by common taxa in the pre-14 ka and post-14 ka, showing a high percentage of positive links in the
951 glacial period (pre-14 ka) while lower in the interglacial period (14-0 ka). Such structures support the
952 stress-gradient hypothesis that positive interactions among organisms become prevalent under
953 stressful environments. Further, more taxa connected via mediators developed a centralized system in
954 the glacial phase. Taxa with Kleinberg's hub centrality score ≥ 0.8 (normalized into an arbitrary range
955 of 0-1 by taking the maximum score into account) are considered keystone taxa and marked in bold.
956 The percentage of positive links has been adjusted to the number of taxa. The chord thickness
957 represents the positive partial correlation.